

REPORT



Off-target binding of an anti-amyloid beta monoclonal antibody to platelet factor 4 causes acute and chronic toxicity in cynomolgus monkeys

Lise I. Loberg^{a#}, Meha Chhaya^b, Alexander Ibraghimov^c, Edit Tarcsa^d, Andreas Striebinger^e, Andreas Popp^f, Lili Huang^b, Frank Oellien^g, and Stefan Barghorn^{e#}

^aDevelopment Sciences, AbbVie Inc., North Chicago, IL, USA; ^bGlobal Biologics, AbbVie Inc., Worcester, MA, USA; ^cPreclinical Safety, AbbVie Inc., Worcester, MA, USA; ^dDMPK-BA, AbbVie Inc., Worcester, MA, USA; ^eDiscovery Biology, AbbVie Deutschland GmbH & Co. KG, Ludwigshafen, Germany; ^fPreclinical Safety, AbbVie Deutschland GmbH & Co. KG, Ludwigshafen, Germany; ^gDiscovery Chemistry, AbbVie Deutschland GmbH & Co. KG, Ludwigshafen, Germany

ABSTRACT

ABT-736 is a humanized monoclonal antibody generated to target a specific conformation of the amyloid-beta (A β) protein oligomer. Development of ABT-736 for Alzheimer's disease was discontinued due to severe adverse effects (AEs) observed in cynomolgus monkey toxicity studies. The acute nature of AEs observed only at the highest doses suggested potential binding of ABT-736 to an abundant plasma protein. Follow-up investigations indicated polyspecificity of ABT-736, including unintended high-affinity binding to monkey and human plasma protein platelet factor 4 (PF-4), known to be involved in heparin-induced thrombocytopenia (HIT) in humans. The chronic AEs observed at the lower doses after repeat administration in monkeys were consistent with HIT pathology. Screening for a backup antibody revealed that ABT-736 possessed additional unintended binding characteristics to other, unknown factors. A subsequently implemented screening funnel focused on nonspecific binding led to the identification of h4D10, a high-affinity A β oligomer binding antibody that did not bind PF-4 or other unintended targets and had no AEs *in vivo*. This strengthened the hypothesis that ABT-736 toxicity was not A β target-related, but instead was the consequence of polyspecificity including PF-4 binding, which likely mediated the acute and chronic AEs and the HIT-like pathology. In conclusion, thorough screening of antibody candidates for nonspecific interactions with unrelated molecules at early stages of discovery can eliminate candidates with polyspecificity and reduce potential for toxicity caused by off-target binding.

ARTICLE HISTORY

Received 9 November 2020
Revised 26 January 2021
Accepted 4 February 2021

KEYWORDS

Antibody biotherapeutic; platelet factor 4; adverse effects; off-target binding; nonspecific binding; polyspecificity; cross-reactivity; heparin-induced thrombocytopenia; amyloid beta; a-beta oligomer

Introduction



Alzheimer's disease (AD), which is the leading cause of dementia among older people, is characterized by the presence of extracellular amyloid plaques and intracellular neurofibrillary tangles in the brain.¹ The amyloid hypothesis of AD assumes that the accumulation of amyloid-beta (A β) peptide in the brain is the primary cause of AD pathogenesis, which results from an imbalance between A β production and A β clearance.^{2,3} Therapeutic approaches for AD include active and passive immunotherapy by developing antibodies that target various forms of A β to lower amyloid levels.

Therapeutic antibodies are designed to have high specificity for the intended target, and therefore little to no side effects are typically observed, other than exaggerated pharmacology. Despite this exquisite specificity, as more antibodies advance into development, multiple reports have described therapeutic antibody candidates binding to unintended targets, resulting in significant toxicity events and/or changes in pharmacokinetics (PK).^{4–7}

ABT-736 is a humanized IgG1 antibody that targets an oligomeric conformation of A β that is present in AD. ABT-736 is the humanized version of m7C6, a mouse monoclonal anti-A β antibody generated against a synthetic antigen

consisting of a truncated A β peptide (A β_{20-42}) in an oligomeric conformation (termed A β_{20-42} globulomer).^{8,9} ABT-736 and m7C6 bind the oligomer with high selectivity compared with other A β conformations such as fibrils or monomer.⁹ Anti-A β antibodies binding to all forms of amyloid fibrils have been associated with the occurrence of microhemorrhages and amyloid-related imaging abnormalities (ARIA).¹⁰ Based on the selectivity of ABT-736 to the oligomeric form of A β , it was expected to be devoid of microhemorrhages and ARIA. ABT-736 and its mouse version m7C6 showed selective target binding toward A β oligomers in *ex vivo* human AD and amyloid precursor protein (APP) transgenic mouse brain experiments. The efficacy of m7C6 was demonstrated in *ex vivo* and *in vivo* APP transgenic mouse model systems.⁹ Thus, ABT-736 was considered for development as a therapeutic for AD. In pre-clinical toxicity studies, high doses of ABT-736 resulted in significant toxicities due to unexpected off-target binding in cynomolgus monkey, but not in a transgenic mouse model of AD.

In this study, we build upon and provide additional details to previous scientific congress reports of the description of the off-target toxicity and identification of platelet factor-4 (PF-4) as the unintended target for ABT-736 likely responsible for the

CONTACT Lise I. Loberg  Lise.loberg@abbvie.com  AbbVie Inc., 1 North Waukegan Road, North Chicago, IL, 60064-6103, USA.

[#]These authors contributed equally to this work.

© 2021 Taylor & Francis Group, LLC

This is an Open Access article distributed under the terms of the Creative Commons Attribution-NonCommercial License (<http://creativecommons.org/licenses/by-nc/4.0/>), which permits unrestricted non-commercial use, distribution, and reproduction in any medium, provided the original work is properly cited.

observed AEs.^{11,12} In addition, we describe *in vitro* screening methods that uncovered additional nonspecific binding activities of ABT-736 and led to the identification of a backup antibody, h4D10. h4D10 had similar affinity to A β , but did not bind PF-4 and also did not demonstrate other unintended binding in *in vitro* screens. Furthermore, h4D10 had no adverse effects in an exploratory toxicity study in cynomolgus monkeys at doses comparable to those that produced toxicity with ABT-736.

Results

The generation of mouse monoclonal antibody m7C6 was previously described;⁹ this antibody and the similarly generated clone m4D10 were humanized as described in Methods. The humanized version of m7C6 is referred to as ABT-736 and the humanized version of m4D10 is referred to as h4D10 in this report. The humanized variants demonstrated comparable affinity to A β as the mouse antibodies (m7C6 and ABT-736: 0.52 nM and 1.56 nM, respectively, with Abeta immobilized, bivalent binding; 4D10 and h4D10: 1.17 and 0.63 nM, respectively, with antibody immobilized, monovalent binding).

ABT-736 PK in cynomolgus monkey

Cynomolgus monkey was selected as a relevant species for toxicity evaluation of ABT-736 based on the identical sequence of A β in cynomolgus monkey and human. Accordingly, ABT-736 would be expected to bind cynomolgus A β oligomer, although high levels of this oligomer would not be expected to be present in normal healthy animals. ABT-736 PK was evaluated in both male and female cynomolgus monkeys, and showed typical monoclonal antibody PK profile with no apparent sex difference (data not shown). Following intravenous (IV) administration at 5 mg/kg the clearance was moderate (0.3 mL/h/kg), volumes of distribution low (V_{ss}: 76.6 mL/kg), and the half-life was somewhat short at 8.8 days. Following subcutaneous (SC) administration (the intended route in the clinic) ABT-736 was absorbed rapidly, reaching maximum serum concentrations at 1.4 days, and had good bioavailability (70.1%).

Severe acute and chronic effects were observed at high doses in cynomolgus monkeys

In a toxicity study, cynomolgus monkeys were to be administered ABT-736 at doses of 20, 60 or 200 mg/kg IV or 60 mg/kg SC weekly for 13 weeks. On the first day of dosing the 20 and 60 mg/kg dose levels were uneventful (n = 5/sex/dose level), whereas the highest dose was not tolerated. A total of four animals were given 200 mg/kg (of planned n = 5/sex); two animals immediately exhibited clinical signs consistent with acute infusion reaction (e.g., irregular respiration, dyspnea, and irregular heartbeat) and died within 10–15 minutes (min) after dosing. The other two animals given 200 mg/kg had similar symptoms, but were stabilized following veterinary treatment with 1,2-dehydrocortisol and etilefrine hydrochloride. One untreated animal was administered a reduced dose of 120 mg/kg and exhibited similar clinical signs, although less

pronounced than at 200 mg/kg, and was removed from the study. None of the surviving animals dosed at 200 mg/kg was given any additional doses, but were kept on study. On Day 12, the surviving two animals of the 200 mg/kg dose group exhibited severe clinical signs, including ataxia, emesis, tremors and/or decreased body temperature, and markedly reduced platelet counts (–34% and –38% compared to baseline); these two animals were subsequently euthanized. Histologic evaluation of tissues from the animals dosed at 200 mg/kg revealed thrombotic changes in the heart, lungs, and/or brain. Microscopic observations included thickening of the artery walls with inflammation in the heart and thrombosis and hemorrhage in the lungs. In one of the animals, hemorrhage was identified in the brain along with degeneration of Purkinje cells in the cerebellum and nerve cells in the occipital neocortex.

The 20 and 60 mg/kg/week dose levels were tolerated to the end of the 13-week dosing and 8-week post-dose recovery periods, but were associated with chronic effects including thrombocytopenia (Figure 1) and vasculature changes (medial hypertrophy and thrombosis), along with neuron loss and microhemorrhages in the brain (Figure 2). Platelet counts decreased compared to baseline levels or the vehicle group and did not recover in the duration between weekly dose administrations. In addition, platelet counts decreased further after dose administration as highlighted by day 84 samples collected immediately or 24 hours after dosing. Platelet counts demonstrated full recovery in all dose groups during the recovery period.

No-Observed-Adverse-Effect level was established in an exploratory monkey toxicity study

To better understand the physiology of the acute infusion reactions and chronic adverse effects observed in the 13-week study, a follow-up investigative study was conducted in cynomolgus monkeys. This study evaluated: 1) whether histopathologic changes in lung and other tissues observed after 13 weeks of

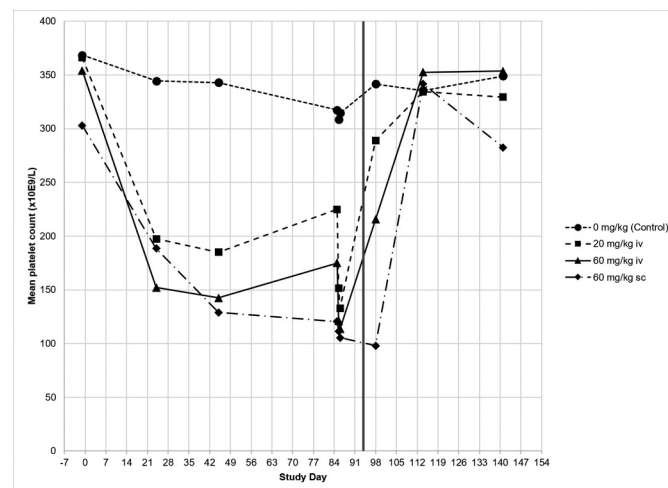


Figure 1. Platelet count in ABT-736 13-week monkey toxicity study. Each line represents the mean of the dose group (n = 10). Vertical line at Day 91 demarcates the beginning of the dose-free recovery period. On Day 84, samples were collected prior to dosing, immediately after dosing, and 24 hours after dosing.

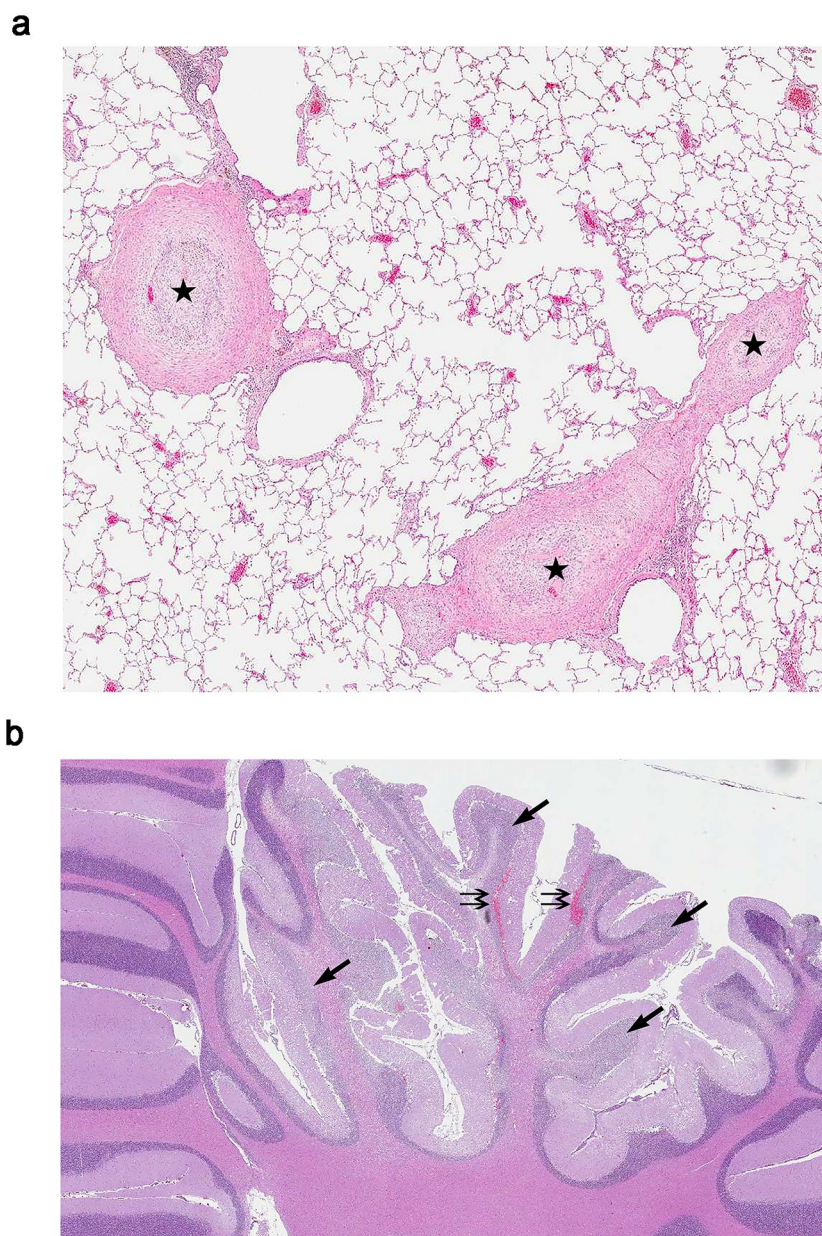


Figure 2. Histological evaluation of cynomolgus monkey tissues. 13 weeks IV administration (once weekly) with 60 mg/kg ABT-736 (a) lung; thrombosis and medial hyperplasia of large lung arteries (star); (b) brain; hemorrhage (double arrows) and degeneration of Purkinje cells and granule cell layer (arrows). Hematoxylin and eosin stain.

dosing would also be observed after a shorter 4-week dose duration at 60 mg/kg by IV bolus injections; 2) cytokine and complement levels; 3) a lower dose level (2 mg/kg); and 4) whether longer IV infusion would ameliorate acute infusion reactions observed at 120 and 200 mg/kg. [Table 1](#) compares the 13-week repeat-dose toxicity study and the 4-week exploratory study, showing a summary of doses, dose routes, and findings for both studies.

Extension of infusion time from bolus injection to 1-hour infusion resulted in milder reactions that were tolerated at both 120 and 200 mg/kg with no changes in physiological indices as measured by implanted telemetry units, but did not ameliorate adverse histopathologic and thrombocytopenia effects. Administration of 120 mg/kg via bolus administration resulted in more severe reactions with ~50% decreases in mean arterial pressure and heart rate.

Complement analyses revealed substantial increases in Bb fragment (3- to 11-fold above baseline) and C3a (4- to 10-fold above baseline) that were dose-related and occurred as early as 5 min post-injection at doses \geq 60 mg/kg, with slight increases in Bb fragment in animals dosed with 2 mg/kg. CH50 was substantially decreased at \geq 120 mg/kg in both bolus and infusion groups, and there was a slight decrease in CH50 at 60 mg/kg. Dose-related increases in the cytokine interleukin-6 (IL-6; 2- to 21-fold above baseline) occurred in all dose groups and were consistent with an inflammatory response. There were no changes in any of the other cytokines evaluated (IL-8, IL-1 β , tumor necrosis factor (TNF), interferon- γ , and granulocyte-macrophage colony-stimulating factor).

Platelet counts decreased (up to 92% compared to baseline) at doses \geq 60 mg/kg at all post-dose time points, with minimal

Table 1. Summary of doses, dose routes and findings in the 13-week repeat dose toxicity study and 4-week exploratory study in monkeys with ABT-736.

Dosage (mg/kg)	Dose route	No. doses	No. animals	Infusion reaction ^a	Complement/Cytokine	Clinical Pathology	Histopathology ^b
13-week repeat-dose study							
20	IV bolus	13	5/sex ^c	NSF	NE	↓ PLT	Thrombi
60	IV bolus	13	5/sex ^c	NSF	NE	↓ PLT	Thrombi
60	SC	13	5/sex ^c	NSF	NE	↓ PLT	Thrombi
120	IV bolus	1	1 (M)	Moderate	NE	NE	NE
200	IV bolus	1	4 (M)	Severe	NE	↓ PLT	Thrombi
4-week exploratory study							
2	IV bolus	4	1/sex	NSF	↑ Bb (slight); ↑ IL6	NSF	NSF
60	IV bolus	4	1/sex	Mild	↑ C3a, Bb; ↓ CH50 (slight); ↑ IL6	↓ PLT	Thrombi
120	IV bolus	1	2/sex	Moderate-Severe; ↓ mAP, HR ^d	↑ C3a, Bb; ↓ CH50; ↑ IL6	↓ PLT	Thrombi
120	IV infusion	4	1/sex	Mild; no changes PI ^d	↑ C3a, Bb; ↓ CH50; ↑ IL6	↓ PLT	Thrombi
200	IV infusion	4	1/sex	Mild-Moderate; no changes PI ^d	↑ C3a, Bb; ↓ CH50; ↑ IL6	↓ PLT	Thrombi

Notes: (a) Infusion reaction observations post-dosing included decreased activity (mild), irregular respiration (moderate), and/or lateral recumbency, irregular heartbeat, and/or mortality/euthanasia (severe). (b) Thrombi: Thrombotic changes in heart, lungs, and/or brain. Heart: thickening of artery walls (medial hypertrophy), inflammation, and thrombosis; lungs: thrombosis and hemorrhage; brain: hemorrhage, degeneration of Purkinje cells and nerve cells. (c) All animals were dosed once weekly for 13 weeks and were evaluated during the dosing period; 3 animals/sex were evaluated for histopathologic effects at the end of the dosing period. (d) Physiological indices (PI) measured by implanted telemetry units.

Abbreviations: No., Number; NSF, No significant findings; NE, Not evaluated; M, male; PLT, platelet; mAP, mean arterial pressure; HR, heart rate; PI, physiological indices

recovery in the 7 days between doses and during the 7 days following the last dose.

Multiple thrombotic lesions and/or arterial changes were observed in lung, injection site and/or brain of animals administered ≥ 60 mg/kg. This study demonstrated that histopathologic effects were observed after 4 weeks of dosing and did not require chronic dosing to manifest.

There were no adverse effects at 2 mg/kg, establishing a No-Observed-Adverse-Effect-Level at this dose level.

The severe acute toxicity observed immediately after dosing only at the highest dose levels implied that ABT-736 may have been binding to an abundant component already present in the circulation, thereby causing the infusion-related effects. It was unlikely that these acute effects were caused by binding the intended A β oligomeric target, since it was expected this was not an abundant circulating protein in normal healthy animals. It was these acute effects that prompted a search to identify a potential cross-reactive antigen to ABT-736.

***In vitro* ABT-736 induced cytokine release and platelet activation**

To dissect the mechanisms underlying the *in vivo* toxicity, *in vitro* characterization of ABT-736 was performed using cytokine release assay and platelet activation (aggregation and/or degranulation) analysis in human and/or monkey.

ABT-736 caused noticeable IL-8 release in diluted whole blood (10%) from untreated cynomolgus monkey (Figure 3a) and healthy human donors (Figure 3b). ABT-736 also elicited release of IL-6 in diluted whole blood from untreated cynomolgus monkey (data not shown). At the same time, cytokine release was not observed when using isolated human peripheral blood mononuclear cells (PBMCs, Figure 3c), suggesting that a non-cellular, soluble factor present in plasma was the mediator necessary for ABT-736 to stimulate cytokine release, likely via immune complex formation. In addition, dose-dependent platelet aggregation was observed in whole blood of cynomolgus monkeys (Figure 4a and b). The observed platelet aggregation could have been induced by ABT-736 binding to a soluble factor and forming immune complexes that might crosslink Fc gamma receptors (Fc γ Rs) on the platelet membrane.

ABT-736 immunoprecipitates PF-4 in human and cynomolgus monkey plasma

Considering the acute toxicity at high doses in the monkey study and the platelet activation that was observed in whole blood, experiments were conducted to confirm that ABT-736 was binding to a soluble protein present in blood and to determine the identity of the protein. ABT-736 immunoprecipitation of cynomolgus monkey serum followed by sodium

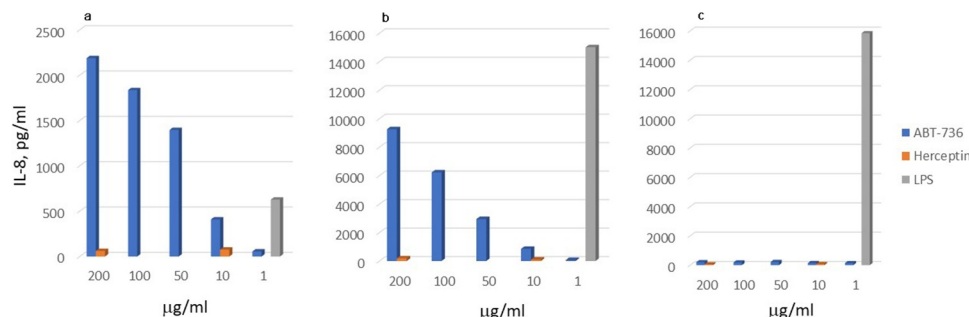


Figure 3. ABT-736 *in vitro* cytokine release. Trastuzumab (human IgG1) is used as a negative control. LPS is used as a positive control. (a) Dose-dependent IL-8 release in whole cynomolgus blood. Representative data of one out of four monkeys shown. (b) Dose-dependent IL-8 release in whole human blood. Representative data of one out of two normal donors shown. (c) Lack of cytokine release by purified human PBMC isolated from normal donor.

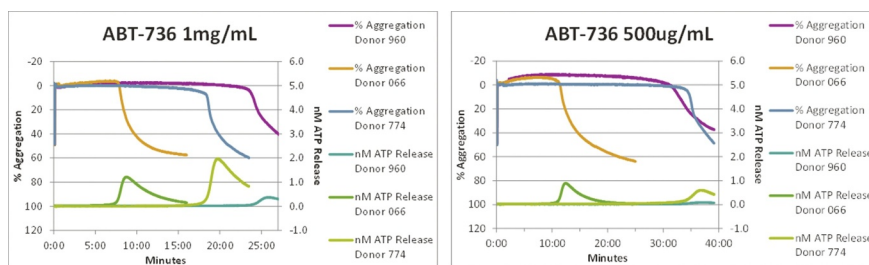


Figure 4. ABT-736 *in vitro* stimulates monkey platelets in a dose-dependent manner. Individual animal platelet activation curves. ABT-736 at a higher concentration of 1 mg/mL (Panel A) in both samples aggregates monkey platelets faster as illustrated by % aggregation (top curves of each plot) and causes degranulation as illustrated by ATP release (bottom curves of each plot) than at lower concentration (500 µg/mL, Panel B).

dodecyl sulfate polyacrylamide gel electrophoresis (SDS-PAGE) showed a specific cross-reactive protein of ~8 kilodaltons (kDa) (Figure 5a). The ABT-736 immunoprecipitate was further analyzed by mass spectrometry and revealed a molecular weight of 8.144 kDa (Figure 5b). Database searches suggested PF-4 as a protein having an identical size (8.144 kDa) in cynomolgus monkey and 7.767 kDa in human. To provide further evidence for PF-4 as the unintended cross-reactive protein, Western blot analysis of ABT-736

immunoprecipitated human and cynomolgus monkey plasma (Figure 5c) were probed with anti-PF-4 antibody. This experiment demonstrated that anti-PF-4 monoclonal antibody stained a protein in the 7–8 kDa range in both monkey and human plasma immunoprecipitates, but not in mouse or rat plasma (data not shown), whereas control mouse IgG2a and/or human IgG1 antibodies stained only unspecific bands. Taken together, these results suggest that ABT-736 exhibits unintended binding to PF-4 in human and monkey plasma.

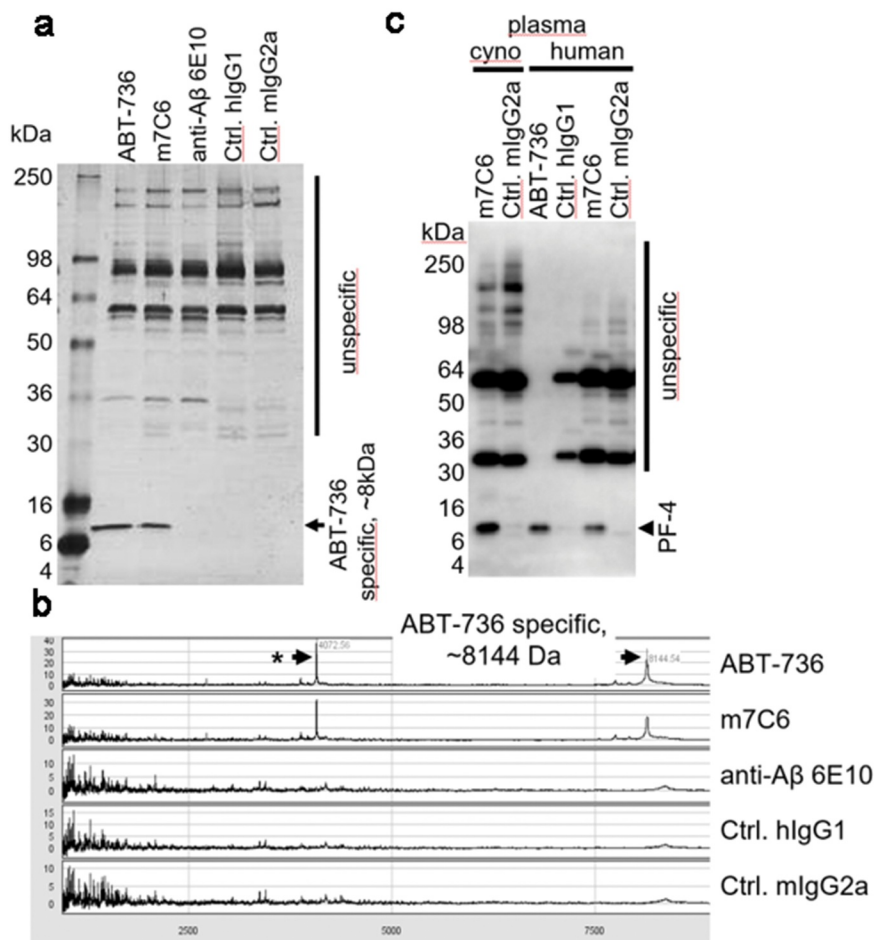


Figure 5. (a) Immunoprecipitation of cynomolgus monkey plasma analyzed via silver-stained SDS-PAGE resulted in a protein-band of approximately 8 kDa, which was specifically immunoprecipitated with ABT-736 and its mouse variant m7C6 but not with the pan-Aβ antibody 6E10 or isotype control antibodies. Note: additional bands at an apparent molecular weight of ~32 kDa and 55 kDa are unspecific bands, as they are present also in the IgG2a negative control and can be attributed to the elution of non-covalently bound antibodies from the immunoprecipitation beads (e.g., m7C6, mlgG2a) and are stained with the anti-mouse detection antibody. (b) SELDI-mass spectrometry analysis of the immunoprecipitates showed similar results and provided a more accurate mass of ~8144 kDa of the cross-reactive protein hinting toward PF-4. (c) Western blot analysis provided further evidence for the ABT-736 PF-4 cross-reactivity in cynomolgus monkey and human plasma.

Identification of anti-A β monoclonal antibody h4D10 with no PF-4 cross-reactivity

A range of anti-A β oligomer antibodies from the same immunization campaign that yielded the mouse variant (m7C6) of ABT-736 showed similar binding characteristics to the A β oligomer and high selectivity compared with other A β conformations such as fibrils or monomer.⁹ To identify antibodies specific for A β oligomer without PF-4 cross-reactivity, a quantitative PF-4 specific enzyme-linked immunosorbent assay (ELISA) assay was established and used as a negative screen for anti-A β oligomer antibodies to avoid cross-reactivity. About half of the tested anti-A β oligomer antibodies demonstrated PF-4 cross-reactivity (9 of 17 tested antibodies bound PF-4 in the ELISA screening assay; data not shown), demonstrating that the unintended binding of ABT-736 to PF-4 was not unique. Nevertheless, a mouse monoclonal antibody m4D10 was identified that did not bind PF-4, and this property was preserved in its subsequently humanized version (Figure 6 a and b). h4D10 showed selective target binding toward A β oligomers in *ex vivo* human AD and APP transgenic mouse brain experiments comparable to ABT-736.⁹ Efficacy of m4D10 was demonstrated in *ex vivo* and *in vivo* APP transgenic mouse model systems. Further screening assays implemented to evaluate *in vitro* cytokine release and *in vitro* platelet activation showed that the backup monoclonal antibody h4D10 did not elicit cytokine response and induced platelet aggregation only after prolonged incubation in one of three cynomolgus monkey whole blood samples (Figure 7, a and b; Table 2). Table 2 compares *in vitro* and *in vivo* data for ABT-736 and h4D10.

PK in rat suggests other nonspecific binding associated with ABT-736, but not with h4D10

ABT-736 and h4D10 contained the same Fc backbone and had similar isoelectric points (pI = 8.5 vs 8.3, respectively), yet when compared in rat PK studies by IV and SC administration, a surprisingly large difference was observed (Figure 8). ABT-736 exhibited relatively high clearance (0.8 mL/h/kg) and short half-life (~5.5 days) with an SC bioavailability of 77.7%. At the same dose, h4D10 exhibited much improved PK properties with reduced clearance (0.25 mL/h/kg), longer half-life (12.2 days) and 100% SC bioavailability.

This relatively large difference in the *in vivo* properties of the antibodies is not due to altered FcRn binding, and could not readily be explained by the observed off-target binding to PF-4 because our experiments demonstrated ABT-736 binding to be specific to monkey and human PF-4 protein only, and not to mouse or rat PF-4.

ABT-736 but not h4D10 exhibits polyspecificity in vitro

To understand the difference between h4D10 and ABT-736 and to evaluate if ABT-736 had broader nonspecific binding characteristics, we established a series of *in vitro* binding assays, including flow cytometry-based cell-binding assays in various cell lines and an ELISA-based baculovirus particle (BVP) assay, and compared ABT-736 and h4D10. ABT-736 showed high nonspecific binding to BVPs by ELISA and to three cell lines tested, including human embryonic kidney (HEK 293G), Chinese hamster ovary (CHO) K1 and monkey

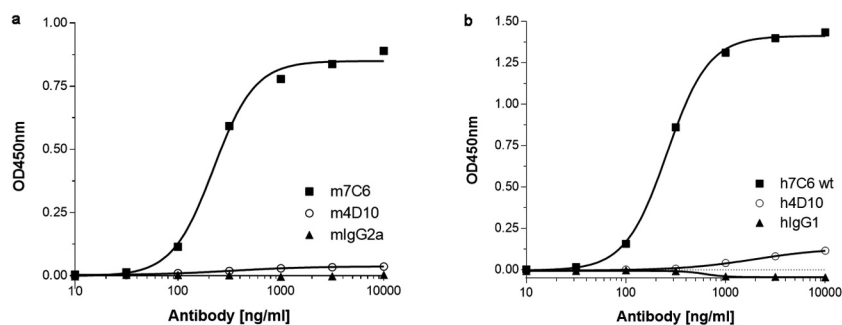


Figure 6. (a) A sandwich ELISA using pooled cynomolgus monkey plasma as a natural source of PF-4 was developed to enable screening for anti-A β oligomer antibodies that were devoid of PF-4 cross-reactivity. The m7C6 antibody used as a positive control shows very strong binding to PF-4 compared to an isotype control antibody and the successfully identified back-up antibody m4D10. (b) Similar results were obtained with the humanized versions of the antibodies (h7C6 and h4D10).

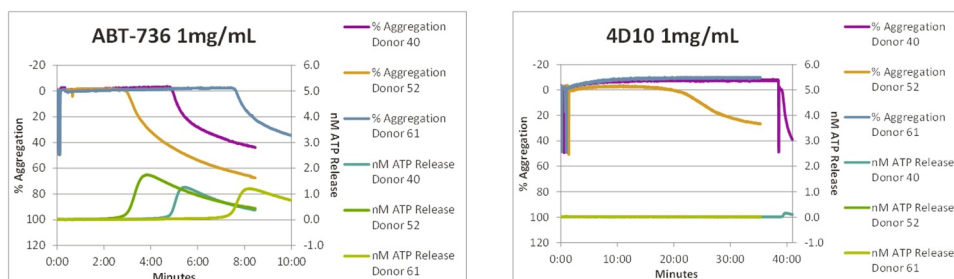


Figure 7. h4D10 does not stimulate monkey platelets. Individual animal platelet aggregation curves. (a) ABT-736 concentration (1 mg/mL) aggregates monkey platelets faster as illustrated by % aggregation (top curves of each plot) than the same concentration of h4D10. (b) h4D10 demonstrates low activity in 1 of 3 samples after a prolonged incubation, compared to high activity in 3 of 3 samples incubated with 1 mg/mL ABT-736.

Table 2. Comparison of ABT-736 and h4D10.

	ABT-736	h4D10
Rat PK (4 mg/kg IV dose)		
Half-life	5.5 days	12.2 days
Clearance	0.8 mL/h/kg	0.25 mL/h/kg
Cytokine release	IL-8	None
Platelet aggregation	Rapid (2–8 min) in 3/3 cyno samples	Slow (20 min) in 1/3 cyno samples
Nonspecific binding to HEK293G/CHO-K1 cells/BVP	Robust Binding	No binding
PF-4 ELISA	Robust binding	No binding
Toxicity findings – acute adverse effects	Rapid infusion related effects and clinical decline	None
Toxicity findings – chronic adverse effects	Thrombocytopenia, thrombosis	None

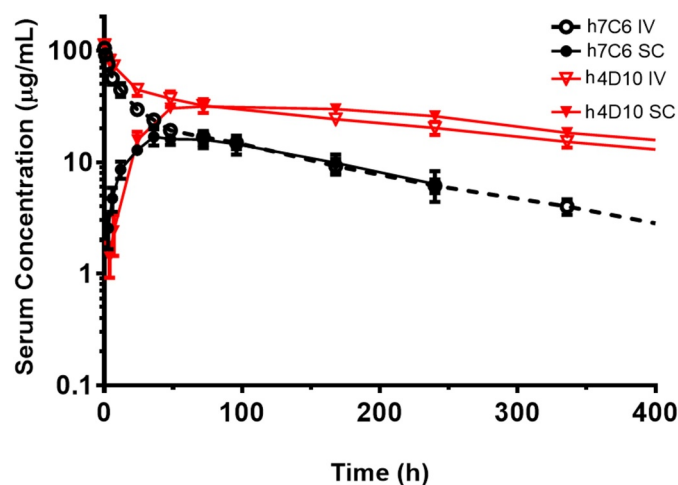


Figure 8. Pharmacokinetic profiles of ABT-736 (h7C6) and h4D10 in Sprague Dawley rat. Mean (\pm SD) serum concentrations of ABT-736 (black circle) or h4D10 (red triangle) following a single 4 mg/kg IV (open symbol) or SC (solid symbol) administration in Sprague Dawley rats ($n = 6$ M/6 F).

kidney COS-7 cells by fluorescence-activated cell sorting (FACS) (Figure 9, a-c). These assays demonstrated that, in addition to relatively specific binding to PF-4, ABT-736 also bound nonspecifically to other components present on the cell surfaces or BVPs. Unintended off-target binding causing unusual PK or adverse events had been described in the literature.^{4–7} In addition, polyreactivity (binding to multiple, unrelated targets) is also a known feature of endogenous antibodies.¹³ In contrast, h4D10 did not exhibit unintended binding to BVPs or any of the cells tested (Figure 9d, Table 2).

Differential binding of ABT-736 versus h4D10 to PF-4 can be rationalized by structural modeling

To rationalize the observed PF-4 binding of half of our anti-A β oligomer antibodies, we crystallized representative examples of each group, and then performed a structure-based analysis of the antigen-antibody interface. We were able to crystallize m4D10 (in-house X-ray, 1.7 Å, data not shown) as a representative of the antibodies without PF-4 binding and m10F11 (m10F11 is a further anti-A β oligomer antibody with comparable A β binding properties and PF-4 cross-reactivity as m7C6; in-house X-ray structure, 2.0 Å, data not shown) as an example

of the Fabs with unintended PF-4 binding. In addition, we created a homology model of m7C6 based on m10F11. A combined sequence and structure-based alignment revealed that the most striking difference between these two antibody populations is the presence of a prolonged loop (7–8 additional amino acids) that is in the center of the antibody-antigen interface and belongs to the heavy chain (Figure 10a/b yellow and orange loop). This loop contains several polar amino acids that seem to be essential for the PF-4 binding. This hypothesis is supported by publicly available Fab-PF-4 complexes described in literature. The KKO Fab (PDB: 4R9Y 1, Figure 10c) as well as the RTO antibody (PDB: 4RAU,¹⁴ Figure 10d) reveal the same prolonged loop in the interface with PF-4. In both cases, polar amino acids in this loop form hydrogen bonds with PF-4 and are essential for PF-4 binding. Loop refinement of the prolonged loops in m10F11 and m7C6 led to similar conformations like the ones in the public structures and are more probable in a complex with PF-4 (Figure 10b).

To analyze the unintended binding of PF-4 to our antibodies in detail, we performed a protein docking of PF-4 (PDB: 1F9Q¹⁴) with antibody m7C6 using Piper (embedded version in Schrödinger Suite 2020–4¹⁵). The best complex model (selected by calculated binding affinity and number of interactions) revealed 4 interactions of the prolonged loop (Ser102, Tyr104 and Tyr107) with PF-4 (Figure 10e). In contrast, the composite model of m4D10 with PF-4 (assuming an identical binding mode of PF-4) showed fewer interactions, including only one interaction with the shortened loop of m4D10, and decreased binding energy (Figure 10f). In addition, the protein-protein interface was significantly reduced because of the shortened loop, leaving a hole in the complex structure (compare Figure 10e and 10f). Taken together the structural modeling data provide a rationale for the unintended binding of ABT-736 to PF-4 and why the back-up antibody m4D10 is devoid of PF-4 binding.

h4D10 had no adverse effects in an exploratory toxicity study in cynomolgus monkeys

The toxicity of h4D10 was evaluated in cynomolgus monkeys at 20 or 100 mg/kg by weekly IV dosing for 4 weeks. There were no adverse clinical observations, no effects on platelet counts, cytokine or complement measurements, and no histopathological changes were observed (Table 3). This study demonstrated no toxicity resulting from administration of an antibody with high affinity to A β oligomer and no evidence for off-target binding, in particular no binding to PF-4, thus strengthening the hypothesis that the toxicity observed with ABT-736 was not target mediated, but likely attributable to PF-4 binding.

Discussion

ABT-736, a humanized monoclonal antibody targeting A β oligomer, was considered for development as a therapeutic for AD. Preliminary tissue cross-reactivity studies were carried out at concentrations up to 10 μ g/mL and demonstrated no noticeable binding of ABT-736 to a panel of normal human or monkey tissues. No side effects were observed in a transgenic

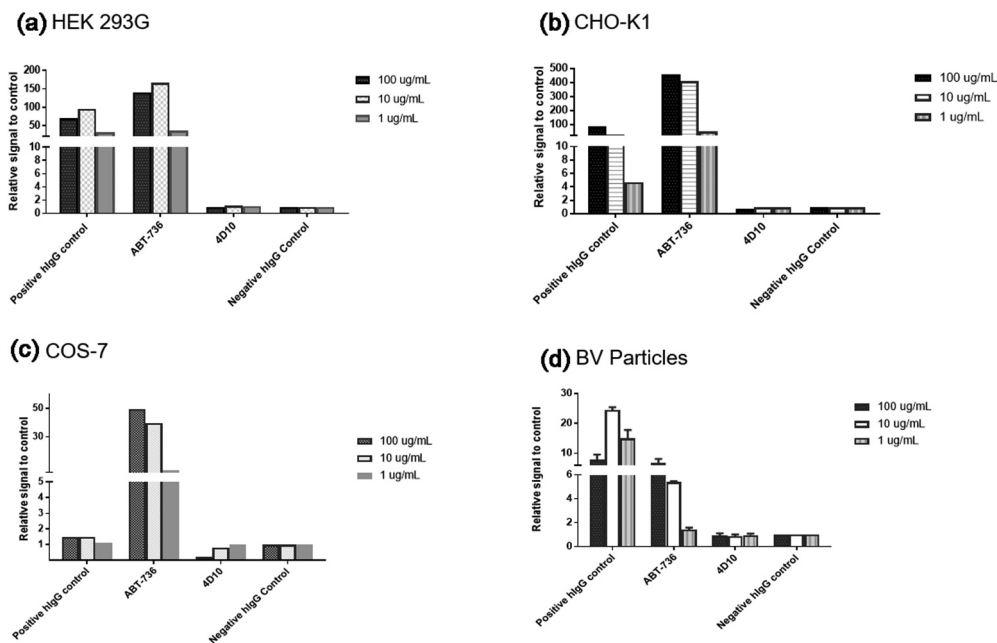


Figure 9. Assessment of off-target binding of human monoclonal antibodies in *in vitro* cell/particle binding assays. Human monoclonal antibodies binding to cells/particles from multiple species. FACS binding of human monoclonal antibodies to (a) HEK 293G cells, (b) CHO-K1 cells, and (c) COS-7 cells. (d) ELISA binding of human monoclonal antibodies to BV Particles. In all the graphs, the Y-axis represents relative signal to control where negative control is 1.

mouse model of AD efficacy or toxicity studies at up to 200 mg/kg for 5 weekly doses, or following a single low-dose (5 mg/kg IV and SC) of ABT-736 in a monkey PK study. PK parameters in cynomolgus monkey were in range with those expected for a human monoclonal antibody, albeit with a somewhat shorter half-life. Based on these data, a 13-week repeat-dose toxicity study of ABT-736 in monkeys was initiated that resulted in serious adverse events. Due to the acute nature of the effects observed at higher doses in monkeys, it was believed that ABT-736 was binding to a blood component to elicit the toxicity. *In vitro* incubations of ABT-736 with isolated human PBMCs showed no cytokine release, but incubations in cynomolgus or human whole blood resulted in cytokine secretion as well as cynomolgus platelet activation, suggesting that a non-cellular, soluble factor present in plasma could be the mediator of the toxicity observed. Immunoprecipitation of ABT-736 with cynomolgus monkey and human blood followed by biochemical characterization identified PF-4, an abundant circulating plasma protein, as a specific binding target of ABT-736 unrelated to A β .

PF-4 is a cytokine that is released from the alpha-granules of activated platelets.^{16,17} It acts as a strong chemoattractant for neutrophils and fibroblasts and is involved in wound repair. PF-4 has a pathological role in heparin-induced thrombocytopenia (HIT) in humans, which is an autoimmune reaction to the administration of the anticoagulant heparin.^{18,19} In HIT, anti-heparin antibodies bind PF-4, forming a complex and resulting in thrombocytopenia and increased thrombosis.²⁰ The acute and chronic thrombotic effects (decreased platelet counts, thromboses observed histologically) in monkeys administered ABT-736 were consistent with HIT pathology in humans. *In vitro* activation and aggregation of platelets in cynomolgus monkey whole blood in the presence of ABT-736 corroborated thrombocytopenia and microthrombi observed

in cynomolgus studies *in vivo*. ABT-736 bound to human and cynomolgus monkey PF-4, but not to mouse PF-4, therefore explaining the differential effects observed in monkey and AD transgenic mouse toxicity studies at comparable dose levels. The unintended binding of ABT-736 to cynomolgus monkey PF-4 could therefore be linked to the toxicities observed in the nonclinical studies in monkeys, and furthermore justified the screen for back-up antibodies that did not bind PF-4.

A backup anti-A β oligomer antibody (h4D10) devoid of PF-4 binding *in vitro* was identified, characterized for nonspecific binding, and evaluated for toxicity in monkeys. There were no adverse effects, including no HIT-like pathology in monkeys administered h4D10 at comparable doses that had produced toxicity with ABT-736. The lack of adverse effects *in vivo* with h4D10 strengthened the hypothesis that the toxicity observed with ABT-736 was not related to A β target, but was off-target, likely PF-4 mediated. Taken together, these experiments demonstrated that ABT-736 specific binding to PF-4 resulted in toxicity in monkeys, leading to termination from further development.

ABT-736 showed no binding to rodent PF-4, yet the *in vivo* rat PK profile with high clearance and short half-life was unusual for a human IgG, especially when compared to h4D10, which has an identical Fc region, comparable pI, and targets the same low abundance soluble protein, oligomeric A β . Since this PK profile in rats could not be attributed to PF-4 binding, other factors such as general polyspecificity were considered as contributing factors to the increased clearance from circulation. *In vitro* assays demonstrated additional off-target binding of ABT-736 in multiple human and rodent cell lines. Polyspecificity has been described for antibodies as the potential of binding multiple unintended targets, usually with lower but measurable affinity. This can be due to the presence of charged or hydrophobic patches in the antibody binding

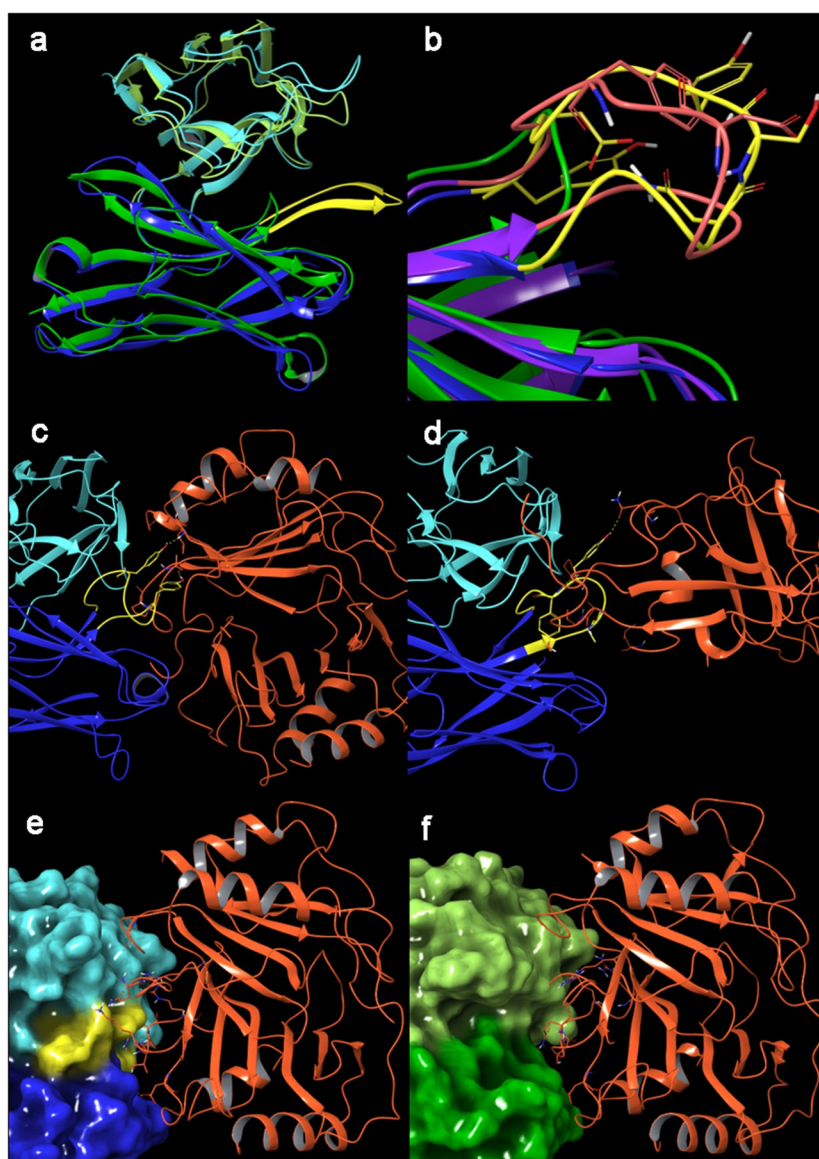


Figure 10. (a) Ribbon representation of X-Ray structures of m10F11 (heavy chain: dark blue, light chain: light blue) and m4D10 (heavy chain: dark green, light chain: light green). The prolonged loop in m10F11 potentially essential for PF-4 binding is highlighted in yellow. (b) Ribbon representation of the heavy chain of m4D10 (green), m10F11 (blue) and m7C6 (purple), the prolonged loop is highlighted in yellow (m4D10) and orange (m7C6), polar amino acids shown as capped sticks. (c, d) Other antibody-PF-4 complexes from the protein database also contain this prolonged loop including polar amino acids interacting with PF-4 (orange); (c) KKOFab (blue/cyan, prolonged loop in yellow, PDB: 4R9Y), (d) RTOFab (blue/cyan, prolonged loop in yellow, PDB: 4RAU). (e, f) Docked and composite model of in-house antibodies with PF-4 (orange); (e) The docked model between m7C6 (blue/cyan; prolonged refined loop in yellow) and PF-4 shows 14 hydrogen bonds in the interface including 4 with the amino acids on the prolonged loop (Ser102, Tyr104 and Tyr107), (f) The composite model of m4D10 (dark and light green) with PF-4 show less interactions (12 hydrogen bonds and only 1 interaction with the shortened loop), reduced binding affinity and a decreased interface caused by a hole established by the missing prolonged loop in m7C6.

Table 3. Summary of 4-week exploratory study in monkeys with h4D10.

Dosage (mg/kg)	Dose route	No. doses	No. animals	Infusion reaction	Complement/Cytokine	Clinical Pathology	Histopathology
20	IV bolus	4	1/sex	NSF	NSF	NSF	NSF
100	IV bolus	4	1/sex	NSF	NSF	NSF	NSF

Abbreviations: No., Number; NSF, No significant findings.

regions.⁷ Depending on the strength of the unintended binding and the abundance of the recognized moieties, these interactions may: 1) have no impact, 2) affect the PK of the antibody, or 3) cause toxicities in severe cases. Polyreactivity is also a known feature of endogenous antibodies, likely related to flexible binding via an induced-fit model.¹³

Interestingly, PF-4, an endogenous protein, also seems to exhibit polyspecific binding. PF-4 is a positively charged protein, released in high quantities at sites of platelet activation where it binds to various negatively charged glycosaminoglycans. In the case of HIT, the basic amino acid residues of PF-4 interact with the negatively charged sulfate groups of heparin,

leading to multimolecular complex formation and severe pathology.²¹ In general, PF-4 appears to be prone to nonspecific interactions, as it has also been described to bind nucleic acids and aptamers.²¹

With respect to the unintended PF-4 binding, our structural modeling data show that ABT-736 exhibits an interaction with PF-4 via a prolonged loop that is absent in h4D10. These data provide a rationale for the unintended binding of ABT-736 to PF-4 and why in contrast h4D10 is devoid of PF-4 binding while maintaining the same A β oligomer binding selectivity and *in vitro* and *ex vivo* efficacy. The unintended binding of ABT-736 to PF-4 led to the toxicity observed in cynomolgus monkeys and eventual termination of ABT-736 from development as a therapeutic for AD. The backup molecule h4D10 was successfully identified as an alternative antibody without PF-4 binding, polyspecificity and with no toxicity observed in cynomolgus monkey studies.

Considering these potential outcomes of nonmechanistic toxicity, it is important to implement tools and assays early in the screening funnel during drug discovery and development to help identify and eliminate high-risk monoclonal antibodies. This would help mitigate late-stage failures due to inadequate exposure or toxicity, thereby increasing the likelihood of success in the clinic.

Materials and Methods

Monoclonal antibody generation and characterization – ABT-736 and h4D10

Mouse monoclonal antibodies (m7C6 and m4D10) were generated by standard *in vivo* immunization of BALB/C mice using A β ₂₀₋₄₂ globulomer antigen, an N-terminal truncated A β oligomer derived by thermolysine limited proteolysis from A β ₁₋₄₂. A β ₁₋₄₂ globulomer was in turn generated from monomeric human A β ₁₋₄₂ synthetic peptide by a multi-step procedure in which 0.2% SDS induced the conformational change to the defined globular oligomer.^{8,9} These antibodies were tested for binding to the selective antigen. The mouse monoclonal antibodies m7C6 and m4D10 were then selected for humanization. The humanized version of m7C6 is referred to as ABT-736 and the humanized version of m4D10 is referred to as humanized 4D10 (h4D10) in this report.

Humanization of mouse antibodies was carried out using complementarity-determining region (CDR) grafting method. CDRs of mouse antibodies were grafted onto the human frameworks. The framework template selection was based upon sequence similarity to close human germline sequences, as well as homology to clinically validated germline sequences. Key murine framework residues that were deemed important in maintaining the integrity of the antigen-binding site were then engineered into the grafted antibody as “back-mutations”. These humanized variable domains were combined with human IgG1/k constant region genes to construct the cDNAs encoding the humanized heavy and light chains. The humanized variants were then characterized for binding potency by competition ELISA with unlabeled mouse antibody as the competitor and for affinity measurement by Biacore.

Animals and husbandry

AbbVie’s laboratory animal programs in general as well as at the local facility where experiments were conducted were accredited by the Association for Assessment and Accreditation of Laboratory Animal Care International during the conduct of the study and all experiments were conducted according to the standards put forth in the National Research Council’s *Guide for the Care and Use of Laboratory Animals*. All study protocols and animal housing and husbandry were approved by the local Institutional Animal Care and Use Committee.

Cynomolgus monkeys (*Macaca fascicularis*) were of Asian origin. All animals were purpose-bred and experimentally naïve at the initiation of the studies.

In vivo toxicity study design

Three repeat-dose toxicity studies were conducted in cynomolgus monkeys: 1) a 13-week study with ABT-736 (Covance Laboratories GmbH, Muenster, Germany), 2) a 4-week investigative study with ABT-736 (Charles River Laboratories, Reno, NV, USA), 3) and a 4-week study with h4D10 (Charles River Laboratories, Reno, NV, USA). ABT-736 and h4D10 were both formulated as an aqueous solution in vehicle containing 31 mM histidine, 8–9% sucrose, and 0.02% polysorbate 80, pH 6.0 for IV or SC injection. In all studies, parameters evaluated included clinical observations, body weights, food consumption, toxicokinetics, clinical pathology (hematology, coagulation, clinical chemistry), cytokine and complement analysis, and anatomic pathology (gross observations, organ weights, histopathology). Additional analyses are described for individual studies.

Study #1: In the 13-week ABT-736 study, monkeys were 3 to 7 years of age at the start of the study and weighed 2.6 to 6.2 kg. Four groups of animals (5/sex/group) received ABT-736 once weekly for 13 weeks at doses of 20 or 60 mg/kg IV (2 mL/kg), 60 mg/kg SC (1 mL/kg), or vehicle control (2 mL/kg IV + 1 mL/kg SC); at the end of the dosing period, 2 animals/sex/group were maintained for an 8-week recovery period. In addition, four males received only a single dose of 200 mg/kg IV (2 mL/kg) and 1 male received a single dose of 120 mg/kg IV (2 mL/kg) due to acute adverse events. Assessment of toxicity was based upon the parameters listed above, as well as cardiovascular examinations (blood pressure and electrocardiograms [ECG]).

Study #2: In the 4-week investigative study, monkeys were approximately 2 to 6 years of age and body weights ranged from approximately 2.5 to 4 kg at the start of the study. The study was divided into two phases: Phase A, which assessed toxicity and histopathologic effects, and Phase B, which assessed acute infusion reactions via implantation of telemetry units. In Phase A, monkeys (1/sex/group) were administered ABT-736 at 0, 2 or 60 mg/kg via IV bolus injection once weekly for four weeks; in this phase, the dose volume was held constant (2.0 mL/kg) and the dose concentration varied accordingly. In Phase B, monkeys (1/sex/group) were administered ABT-736 at 0, 120 or 200 mg/kg via one-hour IV infusion once weekly for four

weeks and another group (2/sex) received 120 mg/kg ABT-736 via IV bolus as a single dose. In Phase B, the dose concentration (100 mg/mL) was held constant and the dose volume varied accordingly. Animals that received 120 mg/kg as a single dose were euthanized and subjected to necropsy on Day 15; all other animals in the study were euthanized on Day 29 at the end of the 4-week repeat dosing schedule. Assessment of toxicity was based upon parameters listed above, with the addition of respiration rate and telemetry parameters for Phase B only (ECG, arterial pressure, heart rate, body temperature).

Study #3: In the 4-week h4D10 study, monkeys were approximately 2 to 3 years of age and body weights ranged from 2.6 to 3 kg. Three groups (1/sex/group) received h4D10 via IV injection once weekly for 4 weeks at 0, 20, or 100 mg/kg (2.33 mL/kg). Assessment of toxicity was based upon parameters listed above.

PK and bioanalysis

The PK properties of ABT-736 and h4D10 were evaluated in Sprague Dawley rats and cynomolgus monkeys following a single IV or SC dose of 4 mg/kg (rat) or 5 mg/kg (monkey). Serum concentrations were measured using an electro chemiluminescent assay employing A β ₂₀₋₄₂ globulomer capture and anti-human Ig detection. Briefly, Mesoscale Discovery (MSD) high bind plates were coated with A β ₂₀₋₄₂ globulomer⁹ at 2 μ g/mL in warm carbonate buffer (37°C) with shaking for 15 min at room temperature (RT) followed by incubation overnight at 4°C. Plates were washed and blocked before samples and standards were diluted in assay buffer, added to plates and incubated for 1 hour (h) at RT. After multiple washes, samples were detected using sulfo-tagged goat anti-human antibody (Meso Scale Discovery, cat. # R32AJ-1). PK parameters were calculated with WinNonlin (Certara v5) via non-compartmental analysis.

Clinical Pathology and Histopathology

Whole blood was collected for hematology evaluation into trisodium citrate anticoagulant and analyzed in an automated blood cell counter (Advia, Bayer Diagnostics).

Tissue samples collected during necropsy were fixed in 10% formalin solution, embedded in paraffin wax and sectioned at nominal 5 μ m and stained with hematoxylin and eosin.

Cytokine release assay

The cytokine release assay was performed with human or cynomolgus monkey whole blood and test article presented in solution. Test article and control antibody [trastuzumab (generated in house)], or lipopolysaccharide (LPS; Sigma, prod. #L-4516) were placed in 48-well plates with samples of peripheral donor blood. Antibodies at a final concentration of 200, 100, 50, 10, and 1 μ g/mL and LPS at a final concentration of 1 μ g/mL were incubated in 500 μ L of 10% diluted blood in RPMI medium with 5% fetal calf serum, for 24 h at 37°C, 5% CO₂. Cells were centrifuged at 1400 RPM for 5 min, supernatants were transferred to 96-well plates and analyzed for

cytokines IL-1ra, IL-1 β , IL-6, IL-8, and TNF (Meso Scale Diagnostics).

Platelet activation analysis

Platelet activation (aggregation and degranulation) was analyzed using protein naïve cynomolgus monkey whole blood and Aggregometer Model 700 (Chrono-log Corp.). Donor blood (405 μ L) was mixed with an equal volume of saline in a cuvette. After 5 min preheat, 90 μ L of luciferase and luciferin (Chrono-LUME reagent, Chrono-log Corp.) was added, followed by addition of the test article(s) at the desired final concentration. Measurement was performed for at least 10 min, followed by adding 4.5 μ L collagen (final concentration 4.5 μ g/mL) to the sample to assess platelets' ability to aggregate and by reading the luminescence to measure released ATP from platelet degranulation.

Immunoprecipitation, SDS-PAGE, mass spectrometry analysis

Preparation of the monkey plasma: A pool of cynomolgus monkey plasma (EDTA plasma pool from 13 different donors) was centrifuged for 10 min at 10,000 g, the cleared supernatant removed and diluted with phosphate-buffered saline with Tween[®] 20 (PBST; 1:10 dilution). Trypsin inhibitor (Sigma cat. no. T7902) was added to a final concentration of 0.1 mg/mL, incubated for 10 min at RT and the sample filtrated through a 0.22 μ m filter (Millipore cat. no. SLGS0250S).

Immunoprecipitation: To identify a potential cross-reactive antigen of ABT-736, a standard immunoprecipitation protocol was applied using pooled monkey plasma. ABT-736 and control-antibodies (mouse monoclonal and humanized antibodies) were captured on anti-mouse IgG or anti-human IgG magnetic beads, respectively. To this end, the beads (Dynabeads M-280 sheep anti-mouse IgG, Invitrogen; Prod. No. 112.02 or Dynabeads M-280 Tosyl-activated, Invitrogen Prod. No. 142.04) coupled with anti-human IgG (according to the manufacturers protocol) were coated with test antibody by overnight incubation at 4°C (at 40 μ g/mL in PBS + 0.1% bovine serum albumin (BSA)). The activated beads were then incubated with the monkey plasma (20 h at 6°C). After washing (twice with PBST, once with 1/10 PBS) bound proteins were eluted from the beads with 50 μ L 0.58% acetic acid, 140 mM NaCl.

SDS-PAGE: For sample preparation the immunoprecipitation eluates (see above) were diluted with 2x Laemmli Buffer + dithiothreitol (1:2). The pH of the samples was carefully neutralized. After heating (5 min at 98°C) the samples were separated on a 4–20% Tris/Glycine Gel at 150 V (4–20% Criterion TGX; 26-well; 1.0 mm; Bio-Rad, cat. no.: 567–1095). Protein bands were visualized by a silver staining procedure according to Blum et al.²²

Western Blot: After separation by SDS-PAGE, the immunoprecipitation eluates were transferred onto PVDF membrane using electrical current. The blots were incubated in PBST with 2% BSA to block nonspecific binding, washed three times each for 10 min with TBST, then incubated with mouse anti-PF-4 antibody (abcam cat. no. ab49735 at

0.2 µg/mL in 3% milk in TBS for 2 h at RT), washed again three times each for 10 min with TBST and incubated with horseradish peroxidase-labeled anti-mouse IgG (1:10000 in 3% milk in TBS for 1 h at RT; Jackson ImmunoResearch Ltd. cat. no.: 715-035-150). After a final washing step for three times each for 10 min with TBST the blots were incubated with a mix of Super Signal West Femto Substrate Enhancer and Peroxide Solution (5 min at RT, ThermoScientific cat. no. 34096) and analyzed using a chemoluminescence imaging system (ChemiDoc Imaging System, BioRad).

SELDI-mass spectrometry analysis: For sample preparation, the immunoprecipitation eluates (see above) were diluted with 50% acetonitrile + 0.5% trifluoroacetic acid (TFA; 1:2) and applied to the arrays of an H4-Chip A-H (Bio-Rad, cat.no. C57-30028). Then α -cyano-4-hydroxycinnamic acid (3.3 mg/mL solution in 50% acetonitrile + 0.5% TFA) was applied to the arrays. The protein-bound chips were transferred into the SELDI TOF mass spectrometer (Ciphergen) and the molecular weights were scanned from 500 to 10,000 Da.

BVP assay for polyspecificity screen

BVPs (LakePharma) were immobilized in 384-well ELISA plates (Nunc Maxisorp) by adding 25 µL of 25% BVP suspension in 50 mM sodium carbonate buffer pH 9.6 to each well, allowing the particles to adsorb to the plates overnight at 4°C.²³ The wells were blocked with 100 µL of blocking buffer (PBS containing 5.0% BSA) for 1 h at RT. After rinsing the plates three times with PBS, antibodies serially diluted in assay buffer (PBS containing 1% BSA) were added in duplicate to the ELISA wells (25 µL per well) and incubated for 1 h at RT. Plates were washed 3 times with PBS and 25 µL of 10 ng/mL goat anti-human IgG (Catalog # 109-035-088) conjugated to horseradish peroxidase (Jackson ImmunoResearch) were added to each well. The plates were incubated for 45 min at RT, washed 3 times with PBS followed by the addition of 25 µL of TMB substrate to each well. Reactions were stopped after 15 min by adding 25 µL of 1 M sulfuric acid to each well and absorbances were read at 450 nm. BVP score was calculated based on the optical density determinations of each well, which had been normalized by dividing it by the average signal observed for control wells containing BVP coat plus secondary antibody only.

Flow cytometry-based off-target cell binding assay

HEK 293G, CHO-K1 or COS-7 cells were harvested from T75 flasks and resuspended in FACS buffer (2% BSA in PBS) at 1.6×10^6 cells/mL and 50 µL of cells/well were added to 96-well round-bottom polypropylene plates. The cells were centrifuged at 1100 rpm for 5 min and washed with 150 µL of ice-cold FACS buffer twice. Antibodies serially diluted in ice-cold FACS buffer were added to wells (100 µL/well) and incubated for 1 h on ice. Plates were washed twice with 150 µL/well of ice-cold FACS buffer. After adding 100 µL per well of 1:100 diluted goat anti-huIgG Fc-PE (Jackson, cat #109-116-098, lot: 97773), the plates were incubated for 30 min on ice and then washed 3 times with 150 µL of ice-cold FACS buffer. Cells were resuspended in 100 µL/

well of ice-cold FACS buffer and read on MacsQuant flow cytometer.

ELISA-based screening assay for PF-4 binding

To determine the cross-reactivity of the test-antibodies toward monkey plasma PF-4 a modified sandwich ELISA protocol was applied. Specifically, the ELISA plates (F96 Cert. Maxisorp NUNC-Immuno Plate cat. no. 439454) were coated with anti-mouse IgG (goat anti-mouse Fc specific IgG; Sigma cat. no.: M3534) by overnight incubation at 4°C (100 µL/well at 50 µg/mL) in coating buffer (100 mM sodium hydrogen carbonate; pH 9.6). After wash, the plates were incubated with a dilution series (0–10 µg/mL) of the test-antibodies (2 h at RT), followed by incubation (2 h at RT) with the monkey plasma (pooled monkey plasma (see above) +0.5% BSA) as a natural source of PF-4. After subsequent washes, a detection antibody (pRAb-PF-4, Abcam cat.no. ab9561 100 µL/well at 1 µg/mL in PBST + 0.5% BSA) was added followed by anti-rabbit-POD conjugate (Jackson ImmunoResearch Ltd. cat. no.: 111-036-045). Detection was carried out by colorimetric readout via TMB (Roche Diagnostics GmbH cat. no.: 92817060), after the reaction was stopped with sulfonic acid, the signal was read at 450 nm.

Structural modeling of the antibody PF-4 interaction

All in silico work has been performed by using the advanced Schrödinger Suite 2020–4.²² The in-house X-ray structures of m4D10 and m10F11 and all public X-ray structures used were prepared by using standard settings in the Protein Preparation wizard. The homology modeling for m7C6 and all loop refinements for the prolonged loop was performed by using the ultra-extended loop sampling method. PF-4 docking on m7C6 was performed by using the antibody docking method in the Piper application in the Schrödinger software suite. The three top poses were further analyzed and the one with most hydrogen bonds and the best calculated Prime binding energy was selected. The m4D10-PF-4 composite model was created by structural alignment of m4D10 with the 7C6-PF-4 complex and transfer of the PF-4 pose to form a complex with m4D10. All complexes were minimized by performing a short (200 ps) Molecular Dynamics Simulation-based minimization. Binding energies between the antibodies and PF-4 were calculated by Prime MMGBSA in Maestro.

Acknowledgments

The authors wish to thank the following AbbVie employees for their support: Christine M. Grinnell for the PK analysis, Daniel Serna for cytokine assay and platelet analysis, Charles W. Hutchins and Kenton Longenecker for crystal structure experiments and structural modeling, and Marjoleen Nijssen and Eric A. Blomme for their critical review of the manuscript. The authors would also like to acknowledge Heinz Hillen (former AbbVie employee) for contributions to the conception of this work.

Funding

AbbVie sponsored and funded the studies described; contributed to the design; participated in collection, analysis, and interpretation of data; and

in writing, reviewing, and approval of the final version. All authors are employees of AbbVie and own AbbVie stock.

ORCID

Lise I. Loberg  <http://orcid.org/0000-0002-6478-9480>

Abbreviations

A β , amyloid-beta; AD, Alzheimer's Disease; AE, adverse effects; ARIA, amyloid-related imaging abnormalities; BVP, baculovirus particle; CDR, complementarity-determining region; CHO, Chinese hamster ovary; ECG, electrocardiogram; ELISA, enzyme-linked immunosorbent assay; FACS, fluorescence-activated cell sorting; Fc γ R, Fc gamma receptor; HEK, human epithelial kidney; HIT, Heparin-Induced Thrombocytopenia; IV, intravenous; kDa, kiloDalton; PBMC, peripheral blood mononuclear cell; PF-4, Platelet Factor 4; pI, isoelectric point; PK, pharmacokinetics; RT, room temperature; SC, subcutaneous; SDS-PAGE, sodium dodecyl sulfate polyacrylamide gel electrophoresis; Vss, volume of distribution

References

- Ballard C, Gauthier S, Corbett A, Brayne C, Aarsland D, Jones E. Alzheimer's Disease. *The Lancet*. 2011;377:1019–31. doi:10.1016/S0140-6736(10)61349-9.
- Hardy JA, Higgins GA. Alzheimer's disease: the amyloid cascade hypothesis. *Science*. 1992;256:184–85.
- Hardy J, Selkoe DJ. The amyloid hypothesis of Alzheimer's disease: progress and problems on the road to therapeutics. *Science*. 2002;297:353–56.
- Vugmeyster Y, Szklut P, Wensel D, Ross J, Xu X, Awwad M, Gill D, Tchistiakov L, Warner G. Complex pharmacokinetics of a humanized antibody against human amyloid beta peptide, Anti-Abeta Ab2, in nonclinical species. *Pharm Res*. 2011;28:1696–706. doi:10.1007/s11095-011-0405-x.
- Santostefano MJ, Kirchner J, Vissinga C, Fort M, Lear S, Pan W-J, Prince PJ, Hensley KM, Tran D, Rock D, et al. Off-target platelet activation in macaques unique to a therapeutic monoclonal antibody. *Tox Path*. 2017;40:899–917. doi:10.1177/0192623312444029.
- Everds N, Li N, Bailey K, Fort M, Stevenson R, Jawando R, Salyers K, Jawa V, Narayanan P, Stevens E, et al. Unexpected thrombocytopenia and anemia in cynomolgus monkeys induced by a therapeutic human monoclonal antibody. *Tox Path*. 2013;41:951–69. doi:10.1177/0192623312474727.
- Datta-Mannan A, Lu J, Witcher DR, Leung D, Tang Y, Wroblewski VJ. The interplay of non-specific binding, target-mediated clearance and FcRn interactions on the pharmacokinetics of humanized antibodies. *mAbs*. 2015;7(6):1084–93. doi:10.1080/19420862.2015.1075109.
- Barghorn S, Nimmrich V, Striebinger A, Krantz C, Keller P, Janson B, Bahr M, Schmidt M, Bitner RS, Harlan J, et al. Globular amyloid β -peptide₁₋₄₂ oligomer – a homogenous and stable neuropathological protein in Alzheimer's disease. *J Neurochem*. 2005;95:834–47. doi:10.1111/j.1471-4159.2005.03407.x.
- Hillen H, Barghorn S, Striebinger A, Labkovsky B, Mueller R, Nimmrich V, Nolte MW, Perez-Cruz C, Van Der Auwera I, Van Leuven F, et al. Generation and therapeutic efficacy of highly oligomer-specific β -Amyloid antibodies. *J Neuroscience*. 2010;30(31):10369–79. doi:10.1523/JNEUROSCI.5721-09.2010.
- Racke MM, Boone LI, Hepburn DL, Parsadainian M, Bryan MT, Ness DK, Piroozzi KS, Jordan WH, Brown DD, Hoffman WP, et al. Exacerbation of cerebral amyloid angiopathy-associated microhemorrhage in amyloid precursor protein transgenic mice by immunotherapy is dependent of antibody recognition of deposited forms of amyloid. *J Neurosci*. 2005;25:629–36.
- Almagro JC, Gilliland GL, Breden F, Scott JK, Sok D, Pauthner M, Reichert JM, Helguera G, Andrabí R, Mabry R, et al. Antibody Engineering and Therapeutics. *mAbs*. 2014;6(3):577–618. doi:10.4161/mabs.28421.
- Sewell F, Chapman K, Couch J, Dempster M, Heidel S, Loberg L, Maier C, Maclachlan TK, Todd M, van der Laan JW. Challenges and opportunities for the future of monoclonal antibody development: improving safety assessment and reducing animal use. *mAbs*. 2017;9(5):742–55. doi:10.1080/19420862.2017.1324376.
- Gunti S, Notkins AL. Polyreactive Antibodies: function and Quantification. *J Infectious Disease*. 2015;212(Suppl1):S42–S46. doi:10.1093/infdis/jiu512.
- Berman HM, Westbrook J, Feng Z, Gilliland G, Bhat TN, Weissig H, Shindyalov IN, Bourne PE. The Protein Data Bank. *Nucleic Acids Res*. 2000;28:235–42.
- Schrödinger LLC. Schrödinger Release 2020–4. New York (NY); 2020.
- McManus LM, Morley CA, Levine SP, Pinckard RN. Platelet activating factor (PAF) induced release of platelet factor 4 (PF4) in vitro and during IgE anaphylaxis in the rabbit. *J Immunol*. 1979;123:2835–41.
- Greinacher A, Alban S, Dummel V, Franz G, Mueller-Ekhardt C. Characterization of the structural requirements for a carbohydrate based anticoagulant with a reduced risk of inducing the immunological type of heparin-associated thrombocytopenia. *Thromb Haemost*. 1995;74:886–92.
- Fabris F, Ahmad S, Cell G, Jeske WP, Walenga JM, Fareed J. Pathophysiology of heparin-induced thrombocytopenia: clinical and diagnostic implications – a review. *Arch Pathol Lab Med*. 2000;124:1657–66.
- Kelton JG, Warkentin TE. Heparin-induced thrombocytopenia: a historical perspective. *Blood*. 2008;112:2607–16. doi:10.1182/blood-2008-02-078014.
- Amiral J, Bridey F, Dreyfus M, Vissoc AM, Fressinaud E, Wolf M, Meyer D. Platelet factor 4 complexed to heparin is the target for antibodies generated in heparin-induced thrombocytopenia. *Thromb Haemost*. 1992;68:95–96.
- Jaax ME, Krauel K, Marschall T, Brandt S, Gansler J, Füll R, Appel B, Fischer S, Block S. Complex formation with nucleic acids and aptamers alters the antigenic properties of platelet factor 4. *Blood*. 2013;122:272–81.
- Blum H, Beier H, Gross HJ. Improved silver staining of plant proteins, RNA and DNA in polyacrylamide gels. *Electrophoresis*. 1987;8:93–99.
- Hötzel I, Frank-Peter Theil LJ, Bernstein SP, Deng R, Quintana L, Lutman J, Sibia R, Chan P, Bumbaca D, Paul Fielder PJ, Carter and Robert F. Kelley, A strategy for risk mitigation of antibodies with fast clearance. *MABS*. 2012;4:753–60.